# Electronic structure in gapped graphene with a Coulomb potential

Wei Zhu,[1] Zhengfei Wang,[1] Qinwei Shi,[1,2,*] K. Y. Szeto,[2] Jie Chen,[3,4] and J. G. Hou[1]
[1]*Hefei National Laboratory for Physical Sciences at Microscale, University of Science and Technology of China, Hefei 230026, China*
[2]*Department of Physics, The Hong Kong University of Science and Technology, Clear Water Bay, Kowloon, Hong Kong*
[3]*Electrical and Computer Engineering, University of Alberta, Alberta, Canada T6G 2V4*
[4]*National Research Council/National Institute of Nanotechnology, Alberta, Canada T6G 2M9*
(Received 10 December 2008; revised manuscript received 20 February 2009; published 17 April 2009)

In this paper, we numerically study bound electron states induced by long-range Coulomb impurities in gapped graphene and quasibound states in the supercritical region based on the lattice model. We present a detailed comparison between our numerical calculations and the prediction of quantum electrodynamics 2+1(QED) continuum model. Furthermore, the supercritical charge has been determined by both the lattice model and the continuum model. The numerical results show that the behavior of quasibound state is consistent with the prediction using Fano's formalism.

DOI: 10.1103/PhysRevB.79.155430 PACS number(s): 81.05.Uw, 71.23.−k, 71.55.−i

## I. INTRODUCTION

Graphene, a two-dimensional (2D) hexagonal lattice of carbon atoms, exhibits a special electronic dispersion relation that can be described by electrons behaving as massless relativistic Dirac fermions.[1–3] This description leads to many unconventional phenomena, such as minimal conductivity,[4,5] the Klein paradox,[6] and the Vaselago lensing effect.[7] The special feature of the large "fine structural constant" in graphene not only provides an exciting platform to validate some predictions of quantum electrodynamics (QED) in the strong field but also provides an interesting "strong coupling" 2+1 QED model.[8]

Recently, it was found that a potential induced by substrate can break the chiral symmetry of the massless Dirac equation and generate a gap in the graphene electron spectrum.[9] The gap then suggests that the motion of electrons can be described by the two-dimensional massive Dirac equations. In this paper, we will investigate the electronic structure of gapped graphene with Coulomb-charged impurities because these impurities induce important changes in the electronic structure.[10–14] It was expected that Coulomb-charged impurities in gapped graphene behave the same as heavy atoms in QED theory.

We expect that bound states be induced inside the gap depending on the charge, $Z$, of the impurity. Moreover, when the charge surpasses a supercritical number, $Z_c$, quasibound states can be generated. For the bound state, when its energy is above the midgap, we can obtain its eigenfunction using the Dirac equation with pure Coulomb potential in a continuum model. On the other hand, when its energy is below the midgap, the continuum model cannot be used due to the singularity of the pure Coulomb potential near $r\sim 0$. Using the approach similar to those in QED to treat the finite spatial extension of the nuclear charge, we adopt an approximate method to remove the singularity.[15] Indeed, when one uses continuum model to describes the behavior of electrons in graphene, how to choose a suitable boundary condition at $r\sim 0$ remains an open question. For example, Ref. 16 chose a "zigzag edge" boundary condition to describe the vacuum polarization in gapless graphene, but Ref. 17 used an "infinite mass" boundary condition. However, these complications in the continuum model can be avoided if we use the tight-binding (TB) approach that is a lattice model. In TB model, there is an intrinsic scale set by the lattice cutoff.

In this paper, a large scale numerical calculation based on the Lanczos method[18] is used to investigate the local density of states (LDOS) in the lattice model. By monitoring the evolution of LDOS in the gap, we can determine the relationship between supercritical charge $Z_c$ and the gap width ($M$). We also choose regularized Coulomb potential ($V=-\frac{Z\alpha}{R}$, $R\neq 0$ for $r<R$, and $V=-\frac{Z\alpha}{r}$) to derive an exact expression for the $Z_c$ in the continuum model. A detailed comparison of the numerical results with the exact expression is presented. Moreover, we investigate the properties of quasibound states in supercritical regime as the Coulomb potential $Z$ becomes greater than supercritical charge $Z_c$. It is found that the properties of those quasibound states can be well described by using Fano's formalism.

## II. LATTICE MODEL AND CONTINUUM MODEL

In the following, we consider a single attractive Coulomb impurity placed at the center of a honeycomb lattice in a graphene sheet. The corresponding Hamiltonian in the tight-binding form is

$$H=-t\left(\sum_{i,j} a_i^\dagger b_j+\text{H.c.}\right)+M\sum_i (a_i^\dagger a_i-b_i^\dagger b_i)$$
$$-\frac{Ze^2}{\varepsilon}\sum_i\left(\frac{a_i^\dagger a_i}{r_i^A}+\frac{b_i^\dagger b_i}{r_i^B}\right), \quad (1)$$

where $t=2.7$ eV is the hopping energy between the nearest neighboring atoms. The operators $a^\dagger(a)$ and $b^\dagger(b)$ denote creation (annihilation) of an electron on sublattice $A$ and sublattice $B$, respectively. The first term of the Hamiltonian describes the hopping between the nearest neighboring atoms. The second term is a mass term arising from an on-site energy difference between sublattices $A$ and $B$. The parameter $M$ appears as the mass (or the gap) of the Dirac fermions. This mass term naturally opens a gap of size $2M$ in the band

 

spectrum. Many conditions can lead to a band gap within graphene. For instance, Ref. 9 reports that the SiC substrate can open a gap of ~0.26 eV in a single-layer graphene, which is consistent with the calculation based on the first principles.[19] In our calculations, we select $M$ from $0.05t$ (or 0.13 eV) to $0.10t$ (or 0.27 eV). $Z$ is the impurity strength and $\varepsilon$ is the effective dielectric constant. When the energy level is close to the Dirac point, the Hamiltonian in gapped graphene can be approximated by a continuum model with pure Coulomb potential: $H=\hbar v_F(-i\sigma_1\partial_x - i\sigma_2\partial_y - \frac{Z\alpha}{r}) + M\sigma_3$, where $\sigma_{1,2,3}$ are the Pauli matrices. We can consider $\alpha=\frac{e^2}{\varepsilon\hbar v_F}$ as the "fine-structure constant" in graphene. $v_F=\frac{3}{2}ta$ is the Fermi velocity of graphene and $a=1.42$ Å. $M$ is the mass of the Dirac fermion. Since $v_F$ is sufficiently small compared with the velocity of light in the QED theory, $\alpha$ becomes large. The large fine-structure constant value in graphene leads to the investigation of the perturbation expansion.

## III. BOUND STATES ABOVE THE MIDDLE GAP

In the continuum model, the eigenfunction of the Hamilton operator with a pure Coulomb potential can be described by the confluent hypergeometric function.[16,20] The regularities at $r\to 0$ and $r\to\infty$ require that the confluent hypergeometric functions reduce to polynomials at the same time. As a result, energy of the bound state within the gap $0<E<M$ is given by

$$E_{n,j}=\frac{M\ \mathrm{sgn}(Z\alpha)}{\sqrt{1+\frac{(Z\alpha)^2}{(n+\gamma)^2}}}, \tag{2}$$

where $\gamma=\sqrt{j^2-(Z\alpha)^2}$. Here, $n=0,1,2,\ldots$ and $j=1/2,3/2,\ldots$. $j$ is the isospin-orbital momentum number.[20] We call the region where $\gamma$ is real for all angular momentum channels the nonsupercritical region. We now discuss the variation in the bound-state energy above the midgap as a function of the charge $Z$. From Eq. (2), we see that the energy of the bound state above the midgap is proportional to the gap width, with the lowest bound state ($j=1/2$) reaching the midgap ($E=0.0$ eV) at a critical value $Z\alpha=j=1/2$. For a general $j$, when the charge $Z$ exceeds $j/\alpha$, $\gamma$ becomes imaginary and the solutions of the continuum model with pure Coulomb potential break down. Hence, no bound states exist below the middle of the gap according to the continuum model with a pure Coulomb potential. However, this artifact can be remedied by removing the singular behavior of the pure Coulomb potential.

We show the numerical result of the LDOS spectrum for the bound state above the midgap in Fig. 1. The calculation uses the Lanczos recursive method[21] in the lattice model. In Figs. 1(a)–1(c), we fix the impurity strength at $Z\alpha=0.4$ and vary the gap width ($M$). The lowest bound states ($n=0$ and $j=1/2$) in the gap can be clearly resolved based on the LDOS spectrum. The other bound states are all very close to the edge of the positive-energy continuum and are not clearly distinguishable from the LDOS spectrum. The variation in the energy of the lowest bound state with gap width is shown in Fig. 1(d), where the dotted line corresponds to our numerical simulations in the lattice model. We can compare our numerical results with the predictions of Eq. (2), which is based on the continuum model. The deviation is small at small gap width and becomes larger for large $M$.

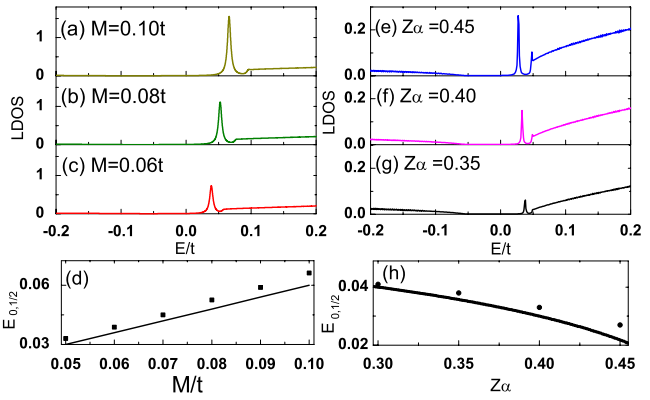


FIG. 1. (Color online) (a)–(c) describe LDOS of the nearest site from the Coulomb impurity with different gaps. (d) shows the relationship between the energy of bound states and the gap when $Z\alpha=0.4$. The line is the theoretical prediction for $Z\alpha=0.4$ and $j=1/2$. (e)–(g) describe the LDOS of the nearest neighbor with different Coulomb charge values at $M=0.05t$. (h) shows the relationship between the energy of bound states and the Coulomb charge values at $M=0.05t$. The black line is the theoretical prediction.

In Figs. 1(e)–1(g), we show the variation in the LDOS spectrum of the bound states with different impurity strength, $Z\alpha$, for fixed gap width at $M=0.05t$. As expected, the peak of the LDOS corresponding to the lowest bound state approaches the midgap as $Z\alpha$ increases. The variation in the energy of the lowest bound state as a function of Coulomb charge is shown in Fig. 1(h). The dotted line gives the result of our numerical simulations, and the fitting curve is plotted using the continuum model. The agreement is again good for small $Z\alpha$. We can see from Fig. 1(h) that the $Z\alpha$ needs to be smaller than 1/2 if the energy of the lowest bound state is above the midgap.

The effect of Coulomb charge on the energy continuum of our gapped graphene is shown in Fig. 2(a). For gapless graphene, our spectrum is qualitatively similar to the spectrum in Ref. 17, where the bound states at $E>3.0t$, and the strong renormalization of the van Hove singularities are mentioned. The major difference shown in our simulations is the bound state in the gap and the dramatic changes in the LDOS near the boundary of the positive continuum when the bound state touches the midgap.

## IV. BOUND STATES BELOW THE MIDDLE GAP

The continuum model of the Dirac equation with the pure Coulomb potential cannot provide the solutions for bound states below the midgap unless suitable boundary conditions are introduced. From our previous discussion, there exists a critical value ($Z\alpha=1/2$) when the lowest bound state touches the midgap. If we use the lattice model, however, we can still obtain the bound states as they gradually enter the energy region below the midgap as $Z\alpha=1/2$ increases beyond 1/2. Here we define in the lattice model a critical value $Z_0\alpha$ that

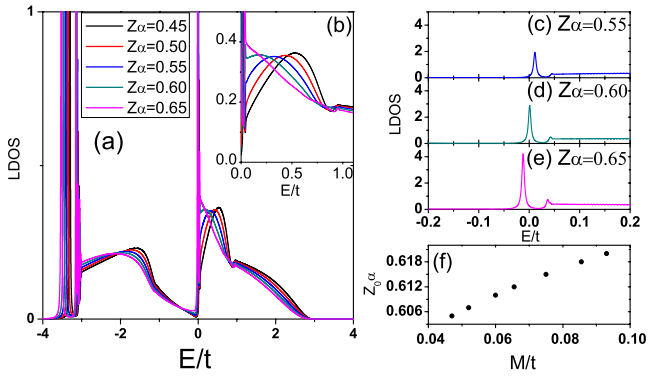


FIG. 2. (Color online) (a) shows the LDOS of the nearest neighboring atoms with different $Z\alpha$ when the gap $M$ is set to be $0.05t$. (b) enlarges the LDOS region as the energy scale $M<E<t$ approaches the midgap. (c)–(e) describe the lowest bound state in the gap for $Z\alpha=0.55$, 0.60, and 0.65, respectively. (f) shows the relationship between critical charge $Z_0\alpha$ and gap width $M$.

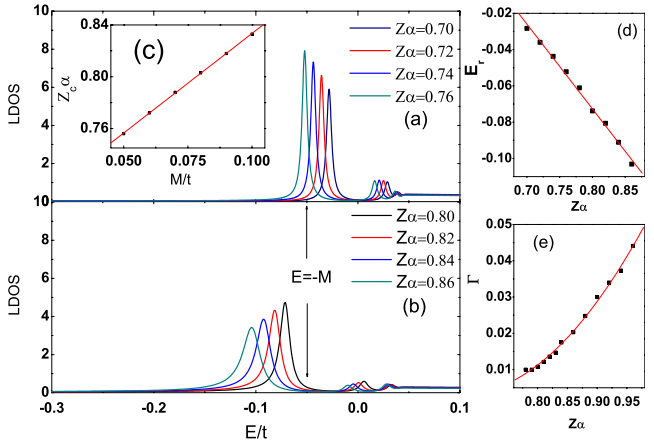


FIG. 3. (Color online) (a) shows the evolving bound states near $E=-M$ when $Z\alpha<Z_c\alpha$. We can observe that LDOS on the bound states becomes larger as $Z\alpha$ increases. (b) describes the evolving resonances near $E=-M$ when $Z\alpha>Z_c\alpha$. The arrow points toward the edge of the gap $E=-M$. Inset (c) shows the relationship between $Z_c\alpha$ and gap width $M$. (d) shows the relationship between the position of resonance $E_r$ and $Z\alpha$. (e) shows the relationship between the width of resonance $\Gamma$ and $Z\alpha$.

corresponds to the energy of the lowest bound state touching the midgap. Near the midgap, we observe some significant change in the LDOS spectrum simulation.

Figure 2(a) shows the LDOS when the bound states enter the region below the midgap for a fixed gap width at $M=0.05t$. These bound states move away from the midgap as $Z\alpha$ increases. The relationship between the critical charge $Z_0\alpha$ and the gap width $M$ is numerically calculated in the lattice model and is shown in Fig. 2(f). Note that this critical value $Z_0\alpha$ depends on the gap width in our lattice model. For example, the critical value $Z_0\alpha$ is about 0.6 when the gap width is $M=0.05t$. (Note that this is different from 1/2 predicted from the continuum model without regularizing the Coulomb potential.[22]) If we carefully look at Fig. 2(b), the resonance peak of the LDOS spectrum in the positive-energy continuum moves toward the edge of the positive continuum as $Z\alpha$ increases. When $Z\alpha=Z_0\alpha$, the peak touches the edge. If $Z\alpha$ increases further, the peak does not move due to the existence of the gap, but the height of the resonance peak increases. These results are similar to those in gapless graphene. We, therefore, believe that the critical value is related to the mechanism that produces the resonance peak at the edge of the positive continuum.

## V. SUPERCRITICAL REGION AND THE DECAY OF VACUUM

As we increase $Z\alpha$ even more, the energy of the lowest bound state approaches the edge of the band gap $(E=-M)$. When $Z\alpha$ is larger than the critical value $Z_c\alpha$, the energy of the bound state will sink into the negative spectrum. In this case, the bound state changes its characteristics and becomes a quasibound state. As predicted by the QED theory,[15] the neutral vacuum will decay into a charged vacuum. The processes of this change is called the decay of vacuum. Here we calculate the supercritical charge $Z_c\alpha$ in gapped graphene in the continuum model as well as the lattice model. First of all, in the continuum model, one needs to remove the singularity of the pure Coulomb potential to determine this critical charge. A simple choice is that the potential takes the form $V=-\frac{Z\alpha}{R}$, $R\neq 0$ for $r<R$, and $V=-\frac{Z\alpha}{r}$ otherwise. On the edge of the overcritical regime, the Dirac wave function can be solved at the point $E=-M$ analytically. Hence, the supercritical charge $Z_c\alpha$ for the lowest bound state can be determined through the boundary condition at $r=R$ (Refs. 15 and 23):

$$\frac{J_1(Z_c\alpha)}{J_0(Z_c\alpha)}=\frac{1}{2Z_c\alpha}\left[1-\rho_c\frac{K'_{i\nu}(\rho_c)}{K_{i\nu}(\rho_c)}\right], \tag{3}$$

where $\rho_c=\sqrt{8MRZ_c\alpha}$ and $\nu=2\sqrt{(Z_c\alpha)^2-j^2}$. $J_l(x)$ is the Bessel function of the first kind and $K_\nu(x)$ is a modified Bessel function. This is a transcendental equation for $Z\alpha$ and the numerical result gives $Z_c\alpha=0.78$ at $MR=0.02$. If the gap width is set to be $M=0.05t$, the corresponding $R$ is approximately $0.6a$.

Next, we consider the lattice model. Figure 3(a) shows the numerical results when the lowest bound state enters the negative-energy continuum. The results indicate that the supercritical charge is about $Z_c\alpha=0.756$ when $M=0.05t$. Inset of Fig. 3(c) reflects the relationship between $Z_c\alpha$ and the gap width $M$ when $R$ is set at $0.6a$. The square dots represent the numerical results based on the lattice model. The fitting line implies that $Z_c\alpha$ depends linearly on the gap width $M$, which satisfies the results derived from the aforementioned transcendental Eq. (4) in the region $0.05t<M<0.10t$. We would like to point out that the relationship between $Z_c\alpha$ and $M$ exhibits a logarithmic singularity when $M\sim 0$, and we have also observed this phenomena as predicted in Ref. 24. However, in this paper, our calculation is in region $0.05t<M<0.10t$ (or $0.13<M<0.26$ eV) which is consistent with the experiment report.[9]

If $Z\alpha>Z_c\alpha$, the lowest bound state enters the negative-energy continuum and becomes a resonant state. We see this trend from the LDOS spectrum shown in Fig. 3(b), where

even the second lowest bound state can be observed. However, the LDOS of quasibound states in the supercritical region decreases as $Z\alpha$ increases and the width of the quasibound state increases with $Z\alpha$ as well. From our numerical results, we find that the position of the resonance peak $E_r=-M+\Delta E$ depends linearly on additional Coulomb charge $\delta Z\alpha=Z\alpha-Z_c\alpha$, while the width of the quasibound state ($\Gamma$) increases quadratically with additional Coulomb charge $\delta Z\alpha$. These observations are qualitatively consistent with the prediction of 3+1 QED based on Fano's formalism used to describe the resonances.[25] The system at the diving point is characterized by a Hamiltonian $H_0(Z\alpha=Z_c\alpha)$. $H_0$ has one discrete eigenstate $|\phi_0\rangle$ with energy $E_0=-M$. Meanwhile $H_0$ has a continuous spectrum when $E<-M$, that is $H_0|\psi_E\rangle=E|\psi_E\rangle$. If the Coulomb impurity charge is larger than $Z_c\alpha$, we consider $V=(Z\alpha-Z_c\alpha)/r=\delta_{Z\alpha}/r$ as a small parameter. Therefore, a wave function satisfied the equation $H|\chi_E\rangle=E|\chi_E\rangle$ in the supercritical regime can be approximately expanded as[25]

$$|\chi_E\rangle = a(E)|\phi_0\rangle + \int dE' b_{E'}(E)|\psi_{E'}\rangle.$$

Here, we assume the function is spanned by the nonperturbation functions $|\phi_0\rangle$ and $|\psi_E\rangle$ (this assumption is correct when the $V$ is weak enough). Our discussion focuses on the edge of the overcritical regime. Our calculation revises the result in Refs. 25 and 26:

$$|a(E)|^2 = \frac{\Gamma/2\pi}{(E-E_0-\Delta E)^2+\Gamma^2/4},$$

where $\Delta E=\delta_{Z\alpha}\langle\phi_0|1/r|\phi_0\rangle$ and $\Gamma=2\pi|V_E|^2=2\pi(\delta_{Z\alpha})^2\langle\varphi_E|1/r|\phi_0\rangle$. On the edge of the overcritical regime, the main term contributed to LDOS $N(\epsilon,r)$ is[16]

$$N(\epsilon,r)=\sum_E |\langle r|\chi_E\rangle|^2\delta(\epsilon-E)\simeq|a(\epsilon)|^2|\langle r|\phi_0\rangle|^2\propto|a(\epsilon)|^2. \tag{4}$$

As a result, the resonance energy $E_r=E_0+\Delta E$ dives linearly with Coulomb charge and the resonance width $\Gamma$ increases quadratically with the Coulomb charge.

Some gedanken experiments were proposed to test the interesting physical processes related to the supercritical vacuum.[15] For example, the dependence of the features of the spectrum of the emitted positron on the "critical duration" reflects the decay of the supercritical vacuum. Unfortunately, there exist many difficulties in performing this experiment in 3+1 QED since the Compton wavelength is very short (0.0004 nm) and fine-structure constant is 1/137. One can expect that the interesting physical processes predicted in QED may be performed in gapped graphene since the fine-structure constant and the corresponding "Compton wavelength $\lambda_g=\hbar V_F/M$" in gapped graphene is sufficiently large compared with those in QED.

## VI. SUMMARY

We have computed numerically the LDOS spectrum using the lattice model for gapped graphene with Coulomb impurities. The results have been compared with the continuum model with pure Coulomb potential. We find that the numerical results can extend the spectrum from the positive to negative spectrum. We also find two critical impurity strength, $Z_0\alpha$ for the lowest bound state touching the midgap ($E=0$) and $Z_c\alpha$ for the entrance to the supercritical region. When $Z\alpha>Z_c\alpha$, the lowest bound state enters the negative-energy continuum and becomes a resonant state. Our numerical work shows that these critical values monotonically increase with the gap width $M$. The width of the quasibound state is explained by Fano's formalism. The many-body effects, such as screening of impurities and renormalization of the gap,[27,28] are under study. We hope our calculations contribute to the future experiment designs.

*Note added*. Recently, we became aware of Ref. 24, which has some overlap with this paper.

## ACKNOWLEDGMENTS

The authors would like to thank Stepan Grinek at the University of Alberta for his valuable input. This work was partially supported by the National Natural Science Foundation of China (Grant No. 10574119). The research was also supported by the National Key Basic Research Program under Grant No. 2006CB922000. K.Y.S. acknowledges the support of CERG under Grants No. 602506 and No. 602507. J.C. would like to acknowledge funding support from the Discovery program of the Natural Sciences and Engineering Research Council of Canada under Grant No. 245680 and the support from the National Institute of Nanotechnology, Canada.

*phsqw@ustc.edu.cn

[1] K. S. Novoselov, A. K. Geim, S. V. Morozov, D. Jiang, Y. Zhang, S. V. Dubonos, I. V. Grigorieva, and A. A. Firsov, Science **306**, 666 (2004).
[2] K. S. Novoselov, A. K. Geim, S. V. Morozov, D. Jiang, M. I. Katsnelson, I. V. Grigorieva, and S. V. Dubonos, Nature (London) **438**, 197 (2005).
[3] A. K. Geim and K. S. Novoselov, Nature Mater. **6**, 183 (2007).
[4] S. Adam, E. H. Hwang, V. M. Galitski, and S. Das Sarma, Proc. Natl. Acad. Sci. U.S.A. **104**, 18392 (2007).
[5] J. H. Chen, C. Jang, S. Adam, M. S. Fuhere, E. D. Williams, and M. Ishigami, Nat. Phys. **4**, 377 (2008).
[6] M. I. Katsnelson, K. S. Novoselov, and A. K. Geim, Nat. Phys. **2**, 620 (2006).
[7] V. V. Cheianov, V. Falko, and B. L. Altsshuler, Science **315**, 1252 (2007).
[8] T. Appelquist, D. Nash, and L. C. R. Wijewardhana, Phys. Rev. Lett. **60**, 2575 (1988).

[9] S. Y. Zhou, G.-H. Gweon, A. V. Fedorov, P. N. First, W. A. Deheer, D.-H. Lee, F. Guinea, A. H. Castro Neto, and A. Lanzara, Nature Mater. **6**, 770 (2007).
[10] T. O. Wehling, A. V. Balatsky, M. I. Katsnelson, A. I. Lichtenstein, K. Scharnberg, and R. Wiesendanger, Phys. Rev. B **75**, 125425 (2007).
[11] A. H. Castro Neto, F. Guinea, N. M. R. Peres, K. S. Novoselov, and A. K. Geim, Rev. Mod. Phys. **81**, 109 (2009).
[12] Yu. V. Skrypnyk and V. M. Loktev, Phys. Rev. B **73**, 241402(R) (2006).
[13] V. M. Pereira, F. Guinea, J. M. B. Lopes dos Santos, N. M. R. Peres, and A. H. Castro Neto, Phys. Rev. Lett. **96**, 036801 (2006).
[14] P. M. Ostrovsky, I. V. Gornyi, and A. D. Mirlin, Phys. Rev. B **74**, 235443 (2006).
[15] W. Greiner and J. Reinhardt, *Quantum Electrodynamics*, 3rd ed. (Springer, New York, 2000).
[16] A. V. Shytov, M. I. Katsnelson, and L. S. Levitov, Phys. Rev. Lett. **99**, 236801 (2007).
[17] V. M. Pereira, J. Nilsson, and A. H. Castro Neto, Phys. Rev. Lett. **99**, 166802 (2007).
[18] S. Wu, L. Jing, Q. Li, Q. W. Shi, J. Chen, H. Su, X. Wang, and J. Yang, Phys. Rev. B **77**, 195411 (2008).
[19] F. Varchon, R. Feng, J. Hass, X. Li, B. Ngoc Nguyen, C. Naud, P. Mallet, J.-Y. Veuillen, C. Berger, E. H. Conrad, and L. Magaud, Phys. Rev. Lett. **99**, 126805 (2007).
[20] D. S. Novikov, Phys. Rev. B **76**, 245435 (2007).
[21] Periodic boundary conditions are used. Typical supercell size in the paper is set to be $L_x=319$ nm and $L_y=369$ nm, enclosing more than $9.0\times10^6$ carbon atoms.
[22] If one introduces a cut-off parameter $R$ to regularize the Coulomb potential, the critical charge $Z_0c$ should depend explicitly on cut-off parameter $R$. Thus, both analytical and numerical calculations should agree.
[23] V. R. Khalilov and C.-L. Ho, Mod. Phys. Lett. A **13**, 615 (1998).
[24] V. M. Pereira, V. N. Kotov, and A. H. Castro Neto, Phys. Rev. B **78**, 085101 (2008).
[25] J. Reinhardt and W. Greiner, Rep. Prog. Phys. **40**, 219 (1977).
[26] B. Muller, H. Peitz, J. Rafelski, and W. Greiner, Phys. Rev. Lett. **28**, 1235 (1972).
[27] M. M. Fogler, D. S. Novikov, and B. I. Shklovskii, Phys. Rev. B **76**, 233402 (2007).
[28] V. N. Kotov, V. M. Pereira, and B. Uchoa, Phys. Rev. B **78**, 075433 (2008).